ORIGINAL RESEARCH

Caspase-1 Inhibition Attenuates Hyperoxia-induced Lung and Brain Injury in Neonatal Mice

Fredrick Dapaah-Siakwan[1,2], Ronald Zambrano[1,2], Shihua Luo[1,2], Matthew R. Duncan[1,2], Nadine Kerr[3,4], Keyur Donda[1,2], Juan Pablo de Rivero Vaccari[3,5], Robert W. Keane[3,4], W. Dalton Dietrich[3,5], Merline Benny[1,2], Karen Young[1,2], and Shu Wu[1,2]

[1]Division of Neonatology and [2]Batchelor Children's Research Institute, Department of Pediatrics, [3]Miami Project to Cure Paralysis, [4]Department of Physiology and Biophysics, and [5]Department of Neurological Surgery, University of Miami Miller School of Medicine, Miami, Florida

ORCID ID: 0000-0002-5233-2117 (S.W.).

Abstract

Hyperoxia plays a key role in the development of bronchopulmonary dysplasia (BPD), a chronic lung disease of preterm infants. Infants with BPD often have brain injury that leads to long-term neurodevelopmental impairment, but the underlying mechanisms that control BPD-induced neurodevelopmental impairment remain unclear. Our previous studies have shown that hyperoxia-induced BPD in rodents is associated with lung inflammasome activation. Here, we tested the hypothesis that hyperoxia-induced lung and brain injury is mediated by inflammasome activation, and that inhibition of caspase-1, a key component of the inflammasome, attenuates hyperoxia-induced lung and brain injury in neonatal mice. C57/BL6 mouse pups were randomized to receive daily intraperitoneal injections of Ac-YVAD-CMK, an irreversible caspase-1 inhibitor, or placebo during exposure to room air or hyperoxia (85% O_2) for 10 days. We found that hyperoxia activated the NLRP1 inflammasome, increased production of mature IL-1β, and upregulated expression of p30 gasdermin-D (GSDMD), the active form of GSDMD that is responsible for the programmed cell death mechanism of pyroptosis in both lung and brain tissue. Importantly, we show that inhibition of caspase-1 decreased IL-1β activation and p30 GSDMD expression, and improved alveolar and vascular development in hyperoxia-exposed lungs. Moreover, caspase-1 inhibition also promoted cell proliferation in the subgranular zone and subventricular zone of hyperoxia-exposed brains, resulting in lessened atrophy of these zones. Thus, the inflammasome plays a critical role in hyperoxia-induced neonatal lung and brain injury, and targeting this pathway may be beneficial for the prevention of lung and brain injury in preterm infants.

Keywords: inflammasome; neonatal lung; brain; hyperoxia; caspase-1

Clinical Relevance

This study demonstrates that inhibition of the inflammasome pathway protects against hyperoxia-induced lung and brain injury in newborn mice. Targeting this pathway may provide a novel therapy for lung and brain injury in preterm infants.

Preterm infants are at great risk of having multiorgan damage that involves the lung and brain (1). Born with immature lungs, these premature infants suffer respiratory failure immediately after birth, and often need respiratory support such as mechanical ventilation and oxygen therapy because their lungs do not have alveoli sufficiently developed for gas exchange (2). However, life-sustaining mechanical ventilation and oxygen therapy can cause lung inflammation that leads

(Received in original form June 7, 2018; accepted in final form January 24, 2019)

Supported by Project Newborn, University of Miami (S.W.); a grant from the March of Dimes Foundation, and a Micah Batchelor Award from the Batchelor Foundation (S.W.).

Author Contributions: Conception and design of the study: F.D.-S., J.P.d.R.V., R.W.K., W.D.D., and S.W. Acquisition, analysis, and interpretation of data: F.D.-S., R.Z., S.L., M.R.D., N.K., K.D., J.P.d.R.V., R.W.K., W.D.D., M.B., K.Y., and S.W. Drafting and editing of manuscript: F.D.-S., M.R.D., J.P.d.R.V., R.W.K., W.D.D., and S.W.

Correspondence and requests for reprints should be addressed to Shu Wu, M.D., Division of Neonatology, Department of Pediatrics, University of Miami Miller School of Medicine, P.O. Box 016960, Miami, FL 33101. E-mail: swu2@med.miami.edu.

This article has a data supplement, which is accessible from this issue's table of contents at www.atsjournals.org.

Am J Respir Cell Mol Biol Vol 61, Iss 3, pp 341–354, Sep 2019

Originally Published in Press as DOI: 10.1165/rcmb.2018-0192OC on March 21, 2019
Internet address: www.atsjournals.org

to damage of alveolar structure. Chronically, inflammation can disrupt lung development by decreasing alveolar and vascular formation, resulting in the neonatal chronic lung disease known as bronchopulmonary dysplasia (BPD) (2, 3). These premature infants also have immature brains that are prone to injurious stimuli such as oxygen toxicity and inflammation. Consequently, they are at greater risk for short-term neurological complications such as intraventricular hemorrhage and encephalopathy of prematurity, and long-term neurodevelopmental sequelae such as cerebral palsy, intellectual disability, and cognitive deficits (4–6). Thus, survivors of BPD not only suffer from long-term pulmonary dysfunction but also often have long-term neurodevelopmental impairment. As such, the cost of treating BPD in the United States is approximately $3 billion a year. The mortality rate for patients with severe BPD complicated by pulmonary hypertension is as high as 50% (7). Despite recent advances in neonatal intensive care and extensive research, the pathogenesis of BPD and brain injury in premature infants is still poorly understood, and there is no effective therapy for these conditions.

There is an increasing recognition of the important role IL-1β plays in the inflammatory pathogenesis of BPD. In clinical studies, increased levels of IL-1β in tracheal aspirates of preterm infants correlated with increased BPD development (8, 9). In experimental models of BPD, treatment with an IL-1 receptor antagonist prevented lung inflammation and injury in newborn mice that were exposed to antenatal inflammation plus moderate postnatal hyperoxia (10). It is known that the cleavage of pro-IL-1β into mature IL-1β is controlled by a multiprotein complex called the inflammasome, which is comprised of NOD-like receptor (NLR) domain-containing proteins (NLRPs), the adaptor protein apoptosis-associated speck-like protein containing a caspase activation recruitment domain (ASC), and caspase-1 (11). The other consequence of inflammasome activation is pyroptosis, an inflammatory form of cell death that is mediated by gasdermin D (GSDMD) (12). A recent study demonstrated that the NLRP3 inflammasome is critically involved in the development of BPD (13). Our previous studies have also shown that exposure of newborn rats to extreme postnatal hyperoxia (85% O_2) activates the NLRP1 inflammasome cascade in the lung, and inhibition of inflammasome protein expression ameliorates hyperoxia-induced neonatal lung injury (14, 15). Moreover, hyperoxia not only can induce lung injury, it can also trigger an inflammatory response in the immature brain, leading to neurodegeneration (16–18). In addition, a recent study demonstrated that caspase-1–processed ILs induced by hyperoxia cause cell death in the developing brain (16). These data highlight a critical role for inflammasome cascades in the pathogenesis of neonatal lung and brain injury. However, the functional mechanisms that control inflammasome pathway regulation of immature lung and brain injury, and their potential as therapeutic targets, remain to be explored.

Hyperoxia-induced neonatal lung and brain injury models in newborn rodents have been widely used for mechanistic studies and to explore potential novel therapies because they share many developmental similarities with preterm infants who are at risk for BPD and brain injury (14–18). Thus, in the present study, we used a newborn mouse model to test the hypothesis that hyperoxia-induced lung and brain injury is mediated by inflammasome activation, and that inhibition of caspase-1, a critical component of the inflammasome cascade, attenuates hyperoxia-induced lung and brain injury in neonatal mice. Here, we report that hyperoxia activated the NLRP1 inflammasome, increased macrophage infiltration, and decreased alveolarization and vascular development in the lung. Similarly, hyperoxia activated the NLRP1 inflammasome, induced cell death, and decreased cell proliferation in the subventricular zone (SVZ) and subgranular zone (SGZ) of the brain. More importantly, our study showed that caspase-1 inhibition by Ac-YVAD-CMK, an irreversible caspase-1 inhibitor (19, 20), downregulated the NLRP1 inflammasome, attenuated lung inflammation, and improved alveolarization and vascular development in the lungs of hyperoxia-exposed mice. Moreover, caspase-1 inhibition decreased pyroptosis-mediated cell death and increased cell proliferation in the SVZ and SGZ in hyperoxic mouse pups. These results suggest that hyperoxia-induced lung and brain injury may be mediated by the NLRP1 inflammasome. As a result, targeting the inflammasome may be beneficial for the prevention of lung and brain injury in preterm infants.

Methods

Detailed descriptions of the materials and methods used in this work are provided in the data supplement.

Animal Model and Experimental Procedure

The Animal Care and Use Committee of the University of Miami Miller School of Medicine approved the experimental protocol. All animals were cared for according to the National Institutes of Health guidelines for the use and care of animals. Newborn C57BL/6 mice were randomized on Postnatal Day 1 (P1) to receive room air (21% O_2) plus placebo (normal saline), room air plus Ac-YVAD-CMK (a selective, irreversible inhibitor of the IL-1β–converting enzyme caspase-1), hyperoxia (85% O_2) plus placebo, or hyperoxia plus Ac-YVAD-CMK. Ac-YVAD-CMK (25 mg/kg) or an equal volume of placebo was administered daily by intraperitoneal injection during continuous exposure to room air or hyperoxia for 10 days. Hyperoxia exposure was achieved in a Plexiglas chamber with continuous O_2 monitoring as previously described (14, 15). On P10, the pups were anesthetized by 0.1% isoflurane, tracheotomized and cannulized, and then killed for analyses.

Caspase-1 Activity Assay

Caspase-1 activity was assessed with 50 μg of protein extract from each lung or brain tissue using a fluorometric kit (R&D Systems) as instructed by the manufacturer.

Analysis of NLRP1 Inflammasome, IL-1β, and GSDMD

Expression of NLRP1, ASC, caspase-1, IL-1β, and GSDMD was assessed by Western blot analysis, and localization of these proteins was determined by immunostaining of tissue sections as previously described (14, 15, 21).

Assessment of Lung Inflammation

Lung inflammation was assessed by immunostaining for MAC-3, a macrophage-

specific marker. The number of MAC-3$^+$ cells in the alveolar air spaces was counted from 10 random images taken with the 20× objective on each slide. Expression of inflammasome proteins, IL-1β and GSDMD was determined by Western blot analysis. Localization of these proteins was determined by immunostaining as previously described (14, 15, 21).

Lung Histology and Morphometry

Lungs were infused with 4% paraformaldehyde via a tracheal catheter at 20 cm H_2O pressure for 5 minutes, fixed overnight, embedded in paraffin wax, and then sectioned. Hematoxylin and eosin staining was performed for lung histology, radial alveolar count (RAC), and mean linear intercept (MLI) measurements as previously described (21).

Measurement of Pulmonary Vascular Density and Vascular Remodeling

Lung sections were immunofluorescently stained for von Willebrand factor (vWF), an endothelial marker. The number of vWF$^+$ vessels (<50 μm in diameter) per high-power field was quantified in five randomly selected, nonoverlapping parenchymal fields on lung sections from each animal. Pulmonary vascular remodeling was assessed by the extent of muscularization of the peripheral pulmonary vessels as previously described (14, 15, 21). Briefly, lung sections were double immunofluorescently stained for vWF and α-smooth muscle actin (α-SMA). Muscularized vessels were defined by the presence of smooth muscle cells that positively stained with α-SMA antibody in 50% or more of the vessel circumference. Ten random, nonoverlapping images on each lung section were viewed and the percentage of muscularized peripheral pulmonary vessels was determined.

Right Ventricular Hypertrophy

Right ventricular hypertrophy, a surrogate marker for pulmonary hypertension, was determined according to the Fulton index, the weight of the right ventricle divided by the left ventricle plus septum (RV/LV+S), as previously described (14, 15, 21).

Preparation of Brain Tissue Sections and Measurement of SVZ and SGZ Volumes

Brain tissues were fixed in 10% formalin, paraffin embedded, and cut serially using a calibrated rotary microtome into 10-μm coronal sections after removal of the olfactory and frontal poles. The sections 1.00 mm from the bregma were stained with hematoxylin and eosin, and four sections from 160 μm to 400 μm were used to measure the SVZ and SGZ surface areas using ImageJ image-processing software. The volumes of the SVZ and SGZ were determined by the product of the surface areas and the thickness of these sections.

Assessment of Cell Death and Cell Proliferation of the SVZ and SGZ

Cell death was studied using a TUNEL assay kit from ThermoFisher Scientific and DAPI blue nuclear stain. The TUNEL assay labels fragmented DNA that results from the programmed cell death that occurs in both apoptosis and pyroptosis. The cell death index was determined by the percentage of TUNEL$^+$ nuclei in the total nuclei in the areas of the SVZ and SGZ. Cell proliferation was assessed by immunofluorescent staining with a rabbit monoclonal anti-Ki67 antibody, a marker for proliferating nuclei, and DAPI blue nuclear stain as previously described (17). The proliferation index was determined by the percentage of Ki67$^+$ nuclei in the total nuclei in the areas of the SVZ and SGZ.

Assessment of Neural Stem Cell Proliferation and Death *In Vitro*

Rat fetal neural stem cells (NSCs) were obtained from Life Technologies and cultured and maintained as recommended by the supplier. Briefly, cells were cultured in Dulbecco's modified Eagle medium/F12 media containing 20 ng/ml epidermal growth factor and basic fibroblast growth factor supplemented with 2% StemPro NSC SFM supplement in tissue culture ware coated with fibronectin. Cells were passaged by accutase treatment and studied between P1 and P4, with cells being >90% positive for the undifferentiated NSC marker nestin. For proliferation and cell death studies, cells were seeded in LabTek slides at 40,000 cells/well and incubated for 6 hours in a normal room air/5% carbon dioxide atmosphere. Cultures were then dosed with placebo (0.25% DMSO/PBS) or AC-YVAD-CMK (25 μg/ml) and half were transferred to a 95% oxygen/5% carbon dioxide atmosphere. After 40 additional hours of culture, the cells were fixed with 4% paraformaldehyde and assays for proliferation (immunofluorescence for Ki67) and cell death (TUNEL assay) were performed.

Data Management and Statistical Analysis

Data were expressed as mean ± SD and comparisons were performed by ANOVA followed by *post hoc* analysis (Student–Newman Keuls). A P value < 0.05 was considered statistically significant.

Results

Ac-YVAD-CMK Inhibits Caspase-1 Activity and Decreases Activation of the NLRP1 Inflammasome in the Lung

We first examined the effect of the administration of Ac-YVAD-CMK, a specific caspase-1 inhibitor, on caspase-1 activity and the expression of NLRP1 inflammasome signaling proteins. As shown in Figure 1, hyperoxia increased caspase-1 activity in the placebo-treated lungs; however, treatment with Ac-YVAD-CMK decreased caspase-1 activity in the hyperoxia-exposed lungs (Figure 1A; there was a 60% increase with O_2 in the placebo group [$P < 0.001$] and this was decreased to 28% in the Ac-YVAD-CMK group [$P < 0.05$]). Hyperoxia also increased the expression of NLRP1, ASC, and active caspase-1 (20 kD subunit) in the placebo-treated mouse pups, but this was significantly decreased in the Ac-YVAD-CMK-treated mice (Figures 1B–1D). Caspase-1 inhibition significantly decreased the production of mature IL-1β (Figure 1E; there was a 2.7-fold increase with O_2 in the placebo group [$P < 0.01$] and this was decreased to 27% by Ac-YVAD-CMK [$P < 0.01$]) and the expression of p30 GSDMD (Figure 1F; there was a 1.2-fold increase with O_2 in the placebo group [$P < 0.05$] and this was decreased to room-air levels with Ac-YVAD-CMK treatment [$P < 0.05$]). Immunohistochemical staining of lung tissue sections showed increased expression of ASC, caspase-1, IL-1β, and

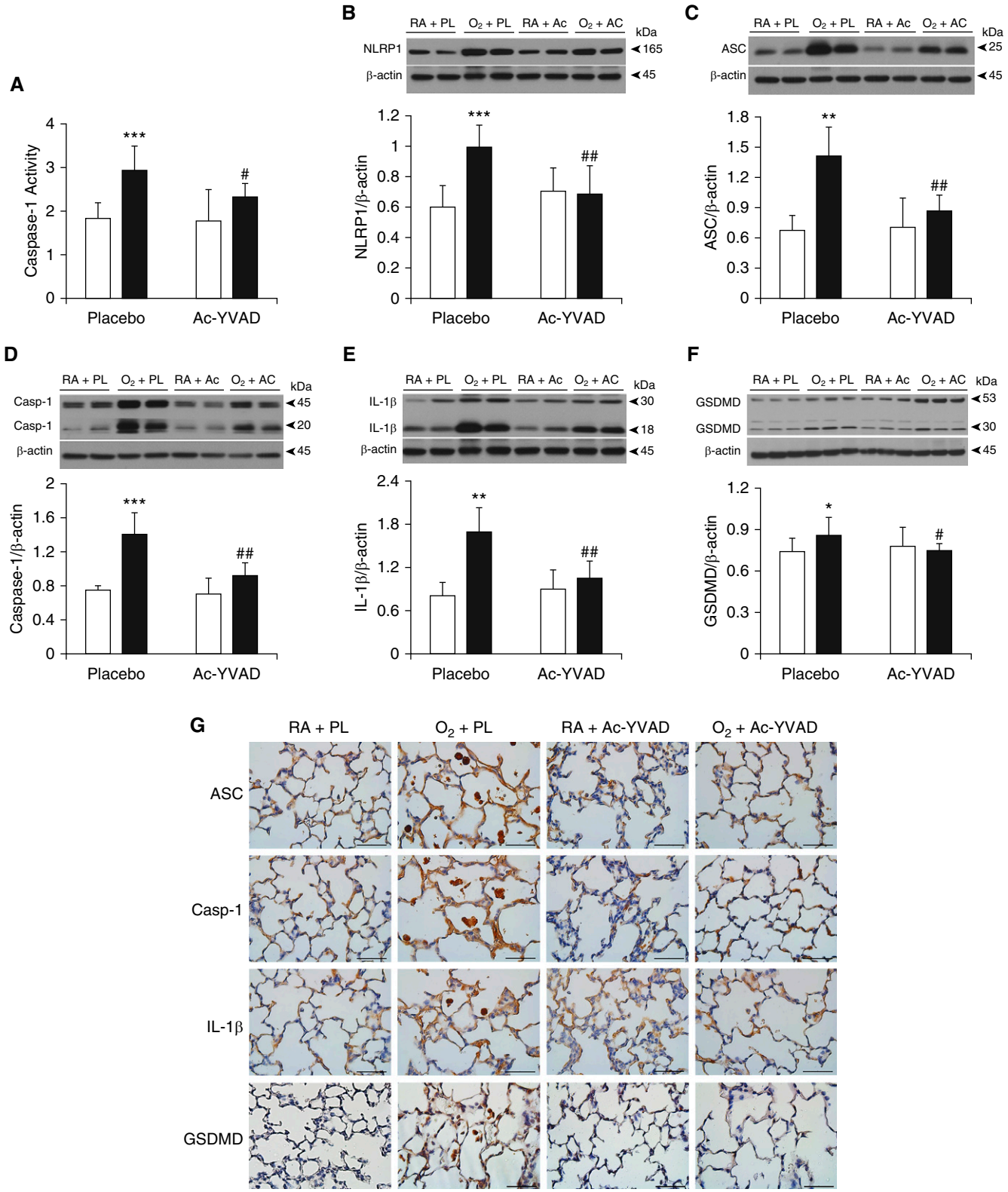

Figure 1. Ac-YVAD-CMK inhibits caspase-1 activity and decreases NLRP1 (NLR family pyrin domain containing 1) inflammasome activation in the lung. Newborn mice were exposed to 85% O_2 from Postnatal Day 1 (P1) to P10 and received a caspase-1 inhibitor, Ac-YVAD-CMK (Ac, Ac-YVAD), or placebo (PL). (*A*) Caspase-1 activity was increased by hyperoxia in the presence of the PL, but treatment with Ac-YVAD-CMK decreased caspase-1 activity in the hyperoxia-exposed lungs. (*B–F*) Western blots show that hyperoxia upregulated expression of NLRP1 (*B*), the adaptor protein apoptosis-associated

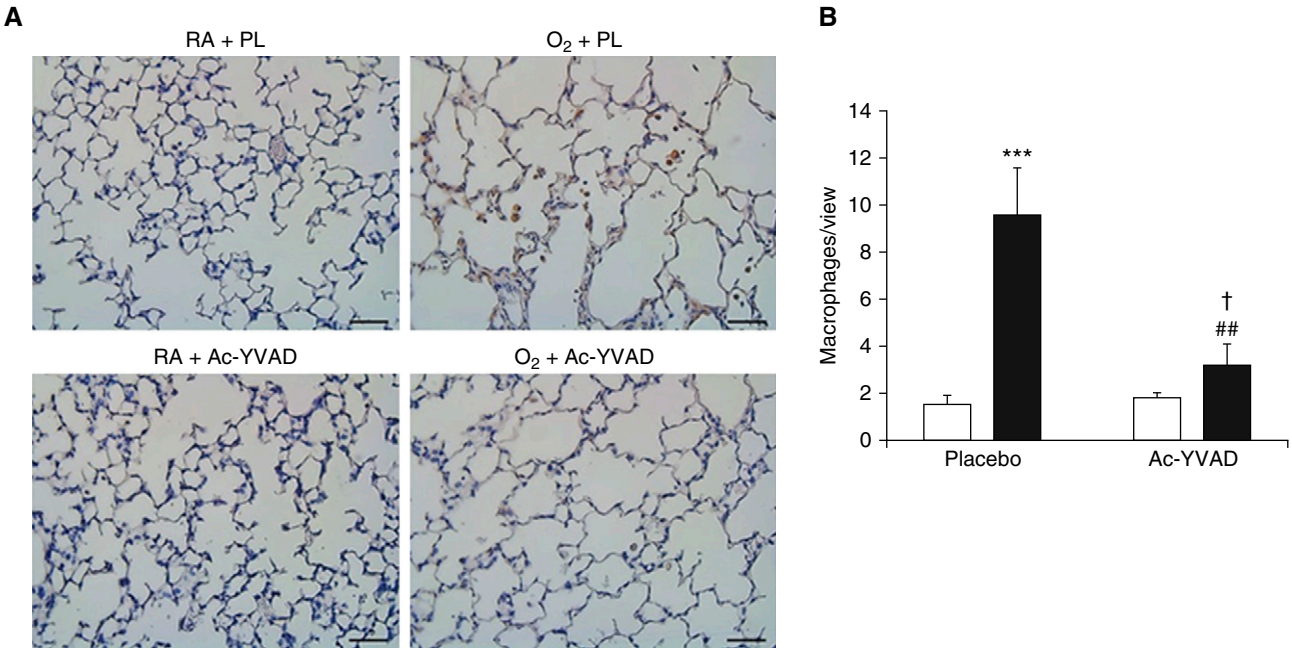

Figure 2. Caspase-1 inhibitor decreases lung inflammation. (*A*) Immunostaining for Mac-3 (macrophage marker, brown signal) showed that hyperoxia increased macrophage infiltration in the presence of the PL. Administration of Ac-YVAD-CMK significantly decreased macrophage counts in the alveolar airspace in hyperoxia-exposed lungs. (*B*) Data are shown as mean ± SD; $n = 4$–6/group. $^{***}P < 0.001$, O_2 + PL versus RA + PL. $^{\#\#}P < 0.01$, O_2 + PL versus O_2 + Ac-YVAD-CMK. $^{\dagger}P < 0.05$, O_2 + Ac-YVAD-CMK versus RA + Ac-YVAD-CMK. Scale bars: 50 μm. Open bar: RA; solid bar: 85% O_2.

GSDMD in placebo-treated mouse pups exposed to hyperoxia, but treatment with Ac-YVAD-CMK decreased the enhanced expression of these proteins in alveolar macrophages (Figure 1G).

Caspase-1 Inhibition Decreases Alveolar Macrophage Infiltration

We next examined whether caspase-1 antagonism could be a strategy to inhibit alveolar macrophage recruitment and infiltration. The hyperoxia-exposed, placebo-treated mouse pups had a more than sixfold increase in macrophage counts compared with the room air–, placebo-treated group (Figures 2A and 2B). However, the administration of Ac-YVAD-CMK significantly decreased macrophage infiltration induced by hyperoxia exposure (Figures 2A and 2B, decreased by fourfold, $P < 0.01$).

Caspase-1 Inhibition Improves Alveolar Development

Next, we studied the effects of caspase-1 inhibition on alveolar development. As shown in Figure 3A, there was no difference in the degree of alveolarization between the groups exposed to room air. Histologically, hyperoxia-exposed animals showed marked simplification of the alveoli as evidenced by larger alveoli with increased alveolar diameters, whereas treatment with Ac-YVAD-CMK increased alveolarization as evidenced by decreased simplification in the treated hyperoxia-exposed group. These observations were quantified by morphometric analysis, which showed decreased RAC (43%, $P < 0.001$) and increased MLI (52%, $P < 0.001$) in the hyperoxia plus placebo group, confirming decreased alveolarization. In contrast, administration of Ac-YVAD-CMK increased RAC (45%, $P < 0.001$) and decreased MLI (33%, $P < 0.01$) in treated hyperoxia-exposed lungs, indicating improved alveolarization as compared with hyperoxia-exposed, placebo-treated lungs (Figure 3B).

Caspase-1 Inhibition Improves Vascular Density and Decreases Vascular Remodeling

The hyperoxia-exposed, placebo-treated group showed a greater than 50% decrease in vascular density compared with the room air–exposed, placebo-treated group (Figures 4A and 4B, $P < 0.001$). However, treatment with Ac-YVAD-CMK significantly increased vascular density by 50% during hyperoxia compared with the hyperoxia-exposed, placebo-treated group (Figures 4A and 4B, $P < 0.001$). Vascular remodeling is a prominent feature of hyperoxia-induced lung injury. Placebo-treated hyperoxic pups had an increased

Figure 1. (Continued). speck-like protein containing a caspase activation recruitment domain (ACS) (*C*), active-caspase-1 (casp-1, 20 kD) (*D*), mature IL-1β (18 kD) (*E*), and p30 gasdermin-D (GSDMD) (*F*) in the presence of the PL. However, treatment with the caspase-1 inhibitor downregulated expression of these factors. Data are shown as mean ± SD; $n = 4$/group. Open bar: room air (RA); solid bar: 85% O_2. (*A*) Caspase-1 activity: $^{***}P < 0.001$, RA + PL versus O_2 + PL; $^{\#}P < 0.05$, O_2 + PL versus O_2 + Ac-YVAD-CMK. (*B*) NLRP1: $^{***}P < 0.001$, RA + PL versus O_2 + PL; $^{\#\#}P < 0.01$, O_2 + PL versus O_2 + Ac-YVAD-CMK. (*C*) ASC: $^{**}P < 0.01$, RA + PL versus O_2 + PL; $^{\#\#}P < 0.01$, O_2 + PL versus O_2 + Ac-YVAD-CMK. (*D*) Active-caspase-1: $^{***}P < 0.001$, RA + PL versus O_2 + PL; $^{\#\#}P < 0.01$, O_2 + PL versus O_2 + Ac-YVAD-CMK. (*E*) Mature IL-1β: $^{**}P < 0.01$, RA + PL versus O_2 + PL; $^{\#\#}P < 0.01$, O_2 + PL versus O_2 + Ac-YVAD-CMK. (*F*) p30 GSDMD: $^{*}P < 0.05$, RA + PL versus O_2 + PL; $^{\#}P < 0.05$, O_2 + PL versus O_2 + Ac-YVAD-CMK. (*G*) Immunostaining showed that 85% O_2 plus the PL increased ASC, caspase-1, IL-1β, and GSDMD expression in alveolar macrophages (brown signal), but treatment with Ac-YVAD-CMK decreased expression of these factors in alveolar macrophages under hyperoxia. Scale bars: 50 μm.

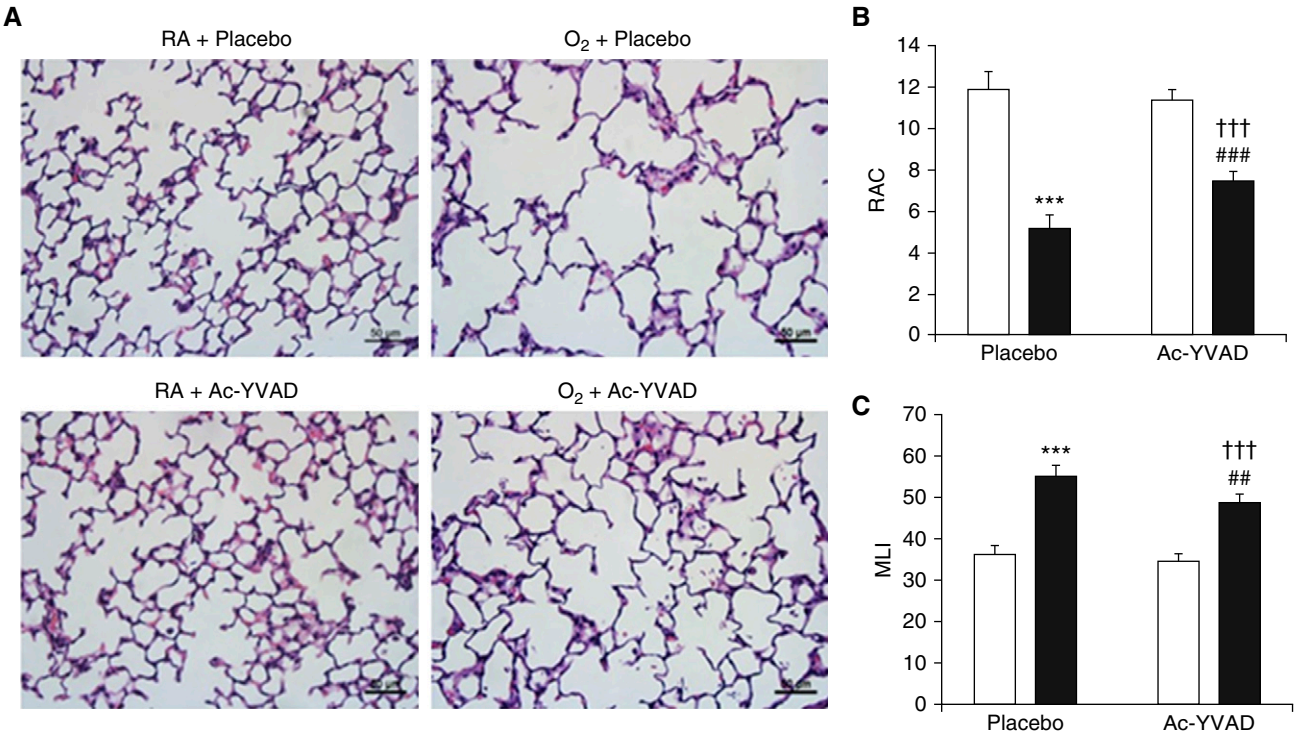

Figure 3. Caspase-1 inhibitor improves alveolarization. (*A*) Hematoxylin and eosin staining shows a larger and simplified alveolar structure in lungs exposed to hyperoxia plus the PL. However, treatment with Ac-YVAD-CMK increased alveolarization of hyperoxia-exposed lungs. Scale bars: 50 μm. (*B* and *C*) Morphometric analysis showed a decreased radial alveolar count (RAC) (*B*) and increased mean linear intercept (MLI) (*C*) in the hyperoxia plus PL group, whereas administration of Ac-YVAD-CMK increased the RAC and decreased the MLI in hyperoxia-exposed lungs. Data are presented as mean ± SD; $n = 4$–8/group. $^{***}P < 0.001$, O_2 + PL versus RA + PL. $^{###}P < 0.001$ and $^{##}P < 0.01$, O_2 + PL versus O_2 + Ac-YVAD-CMK. $^{†††}P < 0.001$, O_2 + Ac-YVAD-CMK versus RA + Ac-YVAD-CMK. Open bar: RA; solid bar: 85% O_2.

percentage of muscularized vessels compared with room air–exposed, placebo-treated pups (Figure 4C, 2.3-fold, $P < 0.001$). In contrast, treatment with Ac-YVAD-CMK significantly decreased the percentage of muscularized vessels during hyperoxia when compared with the hyperoxia-exposed, placebo-treated group (Figure 4C, 75%, $P < 0.001$). Consistent with increased vascular development, the caspase-1 inhibitor also increased expression of vascular endothelial growth factor (VEGF) and VEGF receptor 2 (VEGFR2) (Figures 4D–4F). These results indicate that the inhibition of caspase-1 improves angiogenesis and decreases vascular remodeling during hyperoxia exposure in newborn mice.

Caspase-1 Inhibition Attenuates Hyperoxia-induced Right Ventricular Hypertrophy

Because impaired angiogenesis increases pulmonary vascular resistance, and pulmonary hypertension frequently accompanies BPD, we examined whether caspase-1 inhibition attenuates pulmonary hypertension. We measured Fulton's index, the weight ratio of RV/LV+S, as a surrogate measure of right ventricular hypertrophy. There was a significant increase of RV/LV+S in hyperoxia-exposed, placebo-treated pups as compared with room air–exposed, placebo-treated pups. However, administration of Ac-YVAD-CMK decreased RV/LV+S during hyperoxia exposure (Figure 5; there was a 50% increase in the O_2 placebo group [$P < 0.001$] and this was decreased by Ac-YVAD-CMK treatment to near room-air levels [$P < 0.001$]).

Caspase-1 Inhibition Decreases Activation of the NLRP1 Inflammasome Cascade in the Brain

Because impaired neurodevelopment often accompanies severe BPD, we investigated whether antagonism of caspase-1 during hyperoxia exposure inhibits activation of the NLRP1 inflammasome in the brain. Similar to the results obtained in the lung, hyperoxia increased caspase-1 activity in the placebo-exposed brain, but Ac-YVAD-CMK decreased this activity to near room-air levels (Figure 6A). Hyperoxia also upregulated the expression of NLRP1, ASC, active caspase-1, mature IL-1β, and p30 GSDMD in the presence of the placebo (Figures 6B–6F). However, treatment with Ac-YVAD-CMK downregulated expression of these proteins (NLRP1, 2.5-fold decrease, $P < 0.01$; ASC, 42% decrease, $P < 0.01$; caspase-1, 41% decrease, $P < 0.001$; IL-1β, 54% decrease, $P < 0.01$; p30 GSDMD to room-air levels, $P < 0.01$). Immunostaining of brain tissue sections showed that hyperoxia increased caspase-1, IL-1β, and GSDMD expression in the SGZ, but treatment with the caspase-1 inhibitor decreased the expression of these proteins in the SGZ (Figure 6G).

Caspase-1 Inhibition Decreases Atrophy of the SGZ and SVZ of the Brain

NSCs from the SGZ in the dentate gyrus of the hippocampus and the SVZ in the lateral ventricles continue to proliferate under

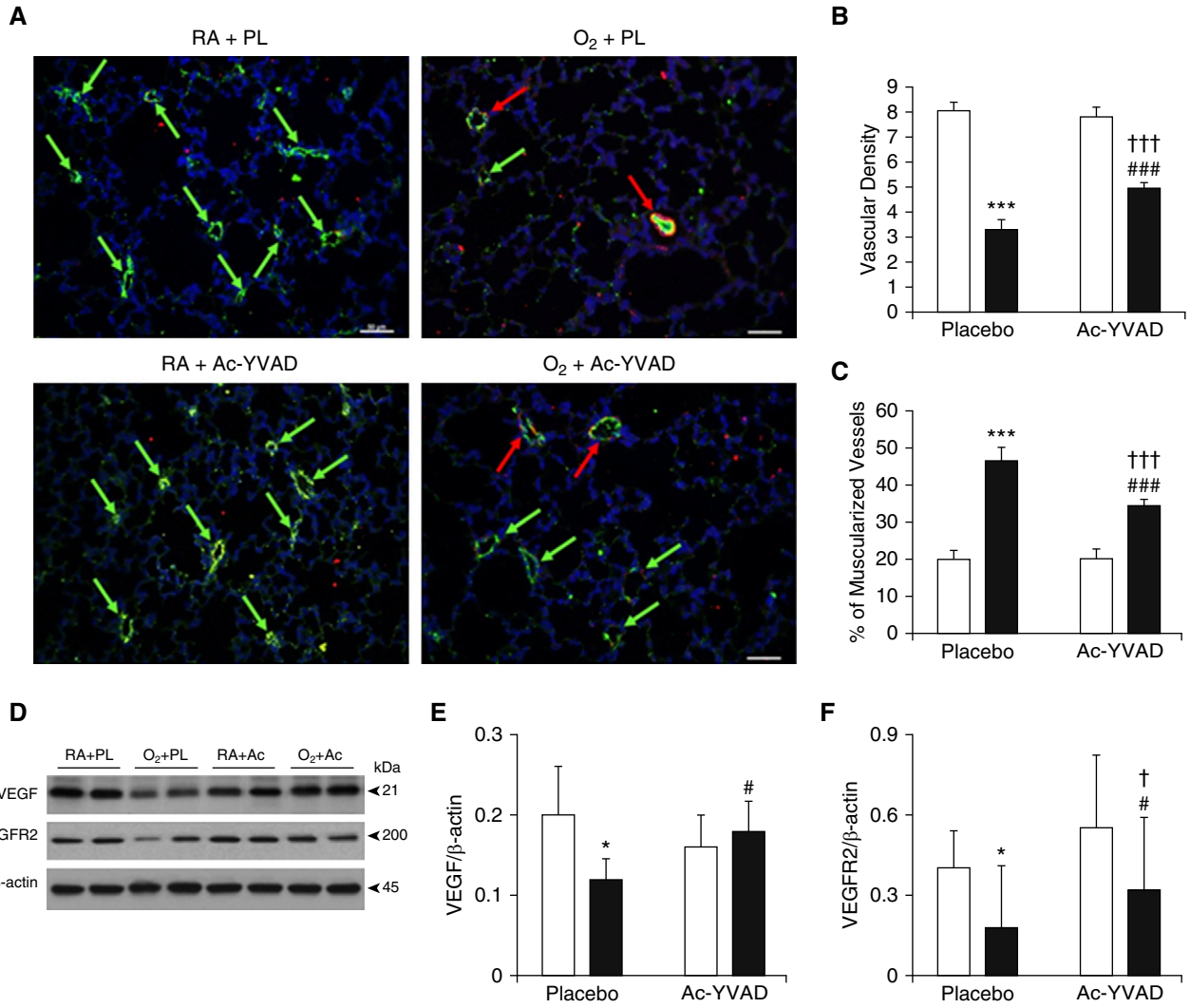

Figure 4. Caspase-1 inhibitor increases vascular development and decreases vascular muscularization. (*A*) Immunofluorescence for von Willebrand factor (an endothelial marker; green), α-smooth muscle actin (α-SMA, a smooth muscle marker; red), and DAPI nuclear stain (blue). Scale bars: 50 μm. (*B*) Vascular densities (vessels < 50 μm, green arrows and red arrows) were decreased in O_2 + PL lungs but were comparatively increased in O_2 + Ac-YVAD-CMK lungs. $^{***}P < 0.001$, O_2 + PL versus RA + PL. $^{\#\#\#}P < 0.001$, O_2 + PL versus O_2 + Ac-YVAD-CMK. $^{\dagger\dagger\dagger}P < 0.001$, O_2 + Ac-YVAD-CMK versus RA + Ac-YVAD-CMK. (*C*) Muscularized vessels (>50% circumference staining for α-SMA, red arrows) were increased in O_2 + PL lungs but were comparatively decreased in O_2 + Ac-YVAD-CMK lungs. $^{***}P < 0.001$, O_2 + PL versus RA + PL. $^{\#\#\#}P < 0.001$, O_2 + PL versus O_2 + Ac-YVAD-CMK. $^{\dagger\dagger\dagger}P < 0.001$, O_2 + Ac-YVAD-CMK versus RA + Ac-YVAD-CMK. Data are presented as mean ± SD; $n = 4$–6/group. Open bar: RA; solid bar: 85% O_2. (*D*) Representative Western blots illustrate that hyperoxia decreased the expression of vascular endothelial growth factor (VEGF) and vascular endothelial growth factor receptor 2 (VEGFR2), whereas their expression was increased by treatment with Ac-YVAD-CMK, as quantitated in *E* and *F*. $^{*}P < 0.05$, RA + PL versus O_2 + PL. $^{\#}P < 0.05$, O_2 + PL versus O_2 + Ac-YVAD-CMK. $^{\dagger}P < 0.05$, O_2 + Ac-YVAD-CMK versus RA + Ac-YVAD-CMK (mean ± SD). $n = 4$–6/group.

normal conditions from birth to throughout adulthood in mammals (16, 17). Previous studies have shown a lower volume and total number of cells in the dentate gyrus, but a higher volume and total cell number in the SVZ in brains exposed to moderate to severe hyperoxia as compared with room air–exposed brains in newborn rats (17). Thus, we sought to determine the effect of caspase-1 inhibition on the development of the SGZ and SVZ during 10 days of hyperoxia exposure. The volume of the SGZ was decreased in the placebo-treated, hyperoxia-exposed group compared with the placebo-treated group exposed to room air, but administration of Ac-YVAD-CMK increased the volume of the SGZ in hyperoxia-exposed brains (Figures 7A and 7B, 69% increase, $P < 0.01$). Similarly, the volume of SVZ was decreased in the placebo-treated hyperoxia-exposed mice, but administration of Ac-YVAD-CMK increased the volume of the SVZ in hyperoxia-exposed brains (Figures 7A and 7C, 35% increase, $P < 0.05$).

Caspase-1 Inhibition Decreases Pyroptosis and Increases Cell Proliferation in Hyperoxia-exposed SGZ and SVZ of the Brain

Given that the hyperoxia-decreased volumes of the SVZ and SGZ could have been due to

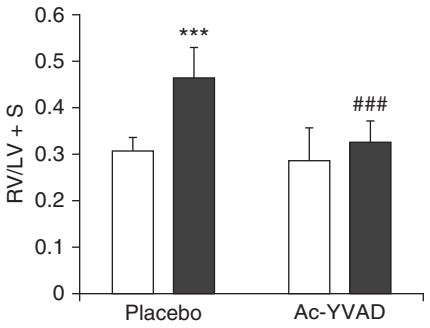

Figure 5. Caspase-1 inhibitor decreases pulmonary hypertension. The Fulton index, the weight ratio of the right ventricle to the left ventricle plus septum (RV/LV+S), was measured to determine right ventricular hypertrophy (RVH), an index for pulmonary hypertension. Hyperoxia with the PL increased RVH as compared with the RA-PL group. However, treatment with Ac-YVAD-CMK decreased RVH to near-RA levels. Data are presented as mean ± SD; $n = 4$–6/group. $^{***}P < 0.001$, O_2 + PL versus RA + PL. $^{\#\#\#}P < 0.001$, O_2 + PL versus O_2 + Ac-YVADYVAD-CMK. Open bar: RA; solid bar: 85% O_2.

programmed cell death (most likely pyroptosis, as GSDMD was also increased by hyperoxia), we measured cell death in the SVZ and SGZ. Quantification of the cell death index (the percentage of $TUNEL^+$ nuclei/total nuclei) in the SVZ revealed that hyperoxia exposure in the presence of the placebo increased cell death. However, treatment with Ac-YVAD-CMK decreased cell death due to hyperoxia (Figures 8A and 8B, 62% decrease, $P < 0.001$). Little cell death was detected in the SGZ of both hyperoxic groups and there was no significant difference between the two groups (data not shown). The presence of the Ki-67 nuclear antigen is a marker of cells in the proliferative phase of the cell cycle (18, 19). Quantification of the proliferation index (the percentage of $Ki67^+$ nuclei/total nuclei) revealed that hyperoxia exposure in the presence of the placebo decreased the proliferation index in the SVZ and SGZ. However, treatment with Ac-YVAD-CMK increased the proliferation index in both the SVZ (Figures 8C and 8D, 86% increase, $P < 0.01$) and the SGZ (Figures 8E and 8F, near room-air levels, $P < 0.01$) during hyperoxia exposure. We further evaluated the effects of Ac-YAAD-CMK on hyperoxia-induced NSC death using cultured NSCs. Exposure to hyperoxia induced greater than 25% cell death in the presence of the placebo, whereas treatment with the caspase-1 inhibitor significantly decreased cell death induced by hyperoxia to 9% (Figure 9B and 9D, $P < 0.01$). In contrast, hyperoxia decreased cell proliferation in the presence of the placebo, but administration of Ac-YVAD-CMK restored cell proliferation by 70% during hyperoxia (Figures 9C and 9E, $P < 0.001$).

Discussion

In the present study, we demonstrate that 10 days of continuous exposure of neonatal mice to hyperoxia led to activation of the NLRP1 inflammasome in the lung and brain, and resulted in the pathological hallmarks of BPD. Caspase-1 inhibition attenuated this hyperoxia-induced NLRP1 inflammasome activation and subsequent pyroptosis-mediated cell death in the lung, and also resulted in improved alveolarization and decreased inflammation in the lungs. Caspase-1 inhibition significantly improved pulmonary vascular development in addition to reducing pulmonary vascular remodeling and right ventricular hypertrophy, a surrogate marker of pulmonary hypertension. The increased expression of NLRP1 inflammasome proteins in the brain during hyperoxia exposure was associated with a reduction in the size and proliferation index of the SVZ and SGZ of the dentate gyrus of the hippocampus, but caspase-1 inhibition attenuated these effects. Collectively, these data suggest that hyperoxia-induced lung and brain injury may be mediated by the NLRP1 inflammasome, and that antagonism of the inflammasome provides a potential therapeutic target for ameliorating the neurodevelopmental impairment that accompanies severe BPD.

One of the key findings of this study is the identification of the NLRP1 inflammasome, IL-1β, and GSDMD cascade as a common pathway that is activated by hyperoxia not only in the lung but also in the brain of neonatal mice. To demonstrate the hyperoxia-induced brain injury that accompanies BPD, we used a well-established hyperoxia-rodent model of BPD that reproduces the histological and physiological phenotype of BPD (14, 15, 21). Other investigators and we have shown that NLRP/IL-1β signaling is critically involved in hyperoxia-induced lung injury in this rodent model of BPD (13–15). In addition, clinical and animal studies have demonstrated increased neutrophils and macrophages in BAL fluid (22, 23) and tracheal aspirates from subjects with BPD (24, 25). In the present study, we found that antagonism of caspase-1 downregulated the expression of the NLRP1 inflammasome proteins, leading to decreased macrophage infiltration in the alveolar spaces of lungs exposed to hyperoxia. This finding is in agreement with the results of a previous study that demonstrated that caspase-1–deficient mice exhibited markedly reduced leukocyte infiltration in the airway after rhinovirus infection (26). The deleterious effects of hyperoxia result from both direct injury mediated by reactive oxygen species (ROS) and indirect injury from lung inflammation (27). Hyperoxia causes cell injury because cellular antioxidant defenses become overwhelmed, leading to the accumulation of toxic levels of ROS and subsequently apoptosis of alveolar epithelial cells (28). Similarly, using an adult mouse model of acute lung injury in which mice were exposed to 100% oxygen, Mantell and colleagues showed that such hyperoxia led to an upregulation of caspase-1 and apoptosis of pulmonary epithelial cells (29).

The mechanism linking hyperoxia to the upregulation of caspase-1 and IL-1β in the pathogenesis of BPD remains unknown. Recent research indicates that mitochondrial ROS production is situated upstream of the NLRP3 inflammasome (30, 31) and that ROS can serve as a redox signaling molecule to activate the NLRP3 inflammasome (32, 33). Furthermore, ROS blockade via chemical scavengers of ROS, as well as pharmacological and genetic inhibition of NADPH oxidase, was shown to suppress inflammasome activation in response to a wide range of stimuli (34, 35). Collectively, our results support the finding that inflammasome-mediated inflammation plays a key role in the pathogenesis of hyperoxia-induced lung injury.

BPD is characterized by alveolar simplification with "dysmorphic" microvasculature and decreased vessel growth (2, 36). In this study, treatment with the caspase-1 inhibitor was not only effective in preventing hyperoxia-induced lung inflammation, it was also beneficial in preventing hyperoxia-induced alveolar structural damage. The inhibition of

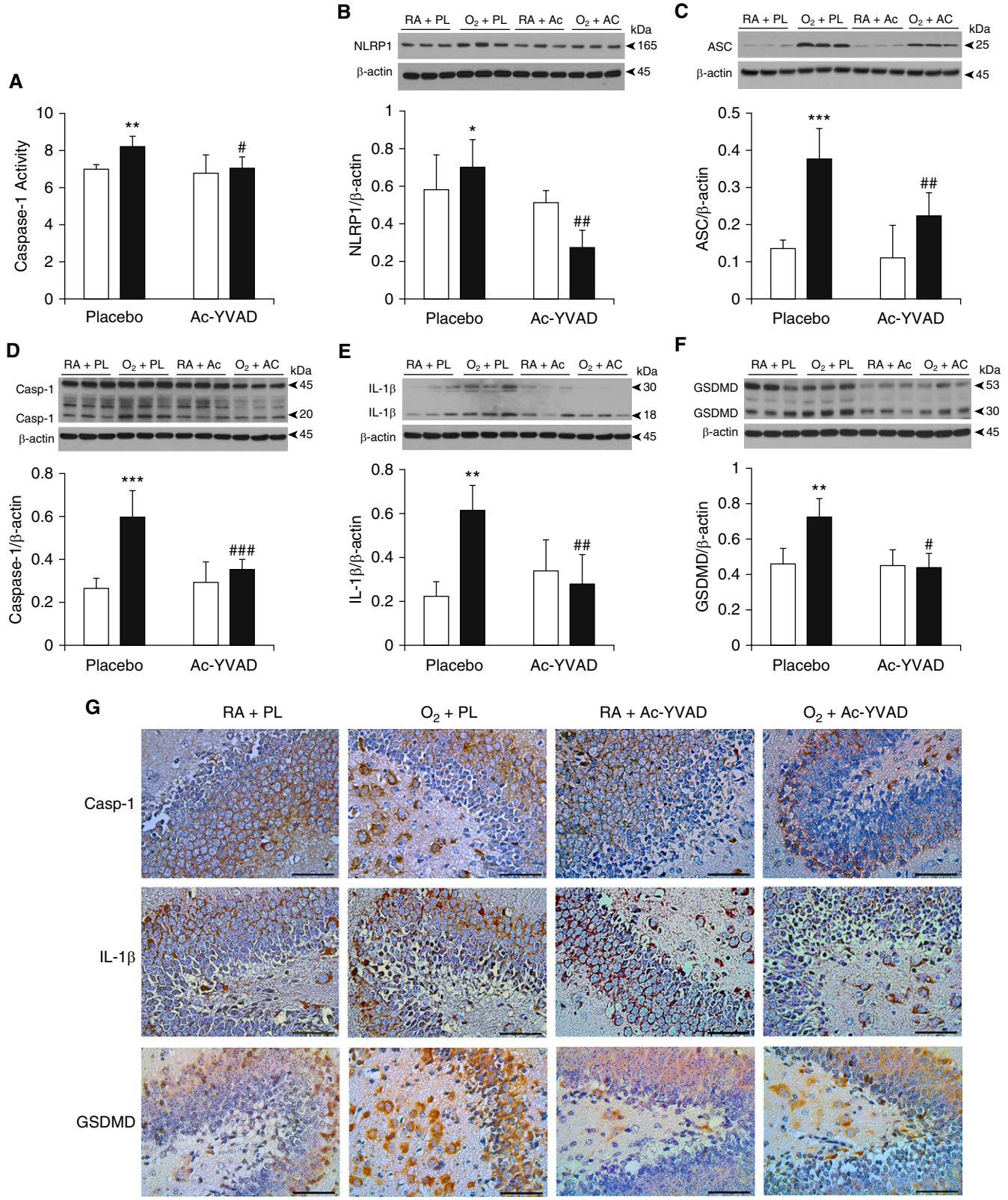

Figure 6. Inhibition of caspase-1 decreases NLRP1 inflammasome activation in the brain. (*A*) Caspase-1 activity was increased by hyperoxia in the presence of the PL, but it was decreased by Ac-YVAD-CMK. (*B–F*) Representative Western blots show that hyperoxia upregulated expression of NLRP1 (*B*), ASC (*C*), active–Casp-1 (20 kD, *D*), mature IL-1β (18 kD, *E*), and p30 GSDMD (*F*) in the presence of the PL. However, treatment with Ac-YVAD-CMK downregulated expression of these proteins. (*A*) Caspase-1 activity. (*B*) NLRP1: $^{*}P < 0.05$, RA + PL versus O_2 + PL; $^{\#\#}P < 0.01$, O_2 + PL versus O_2 +

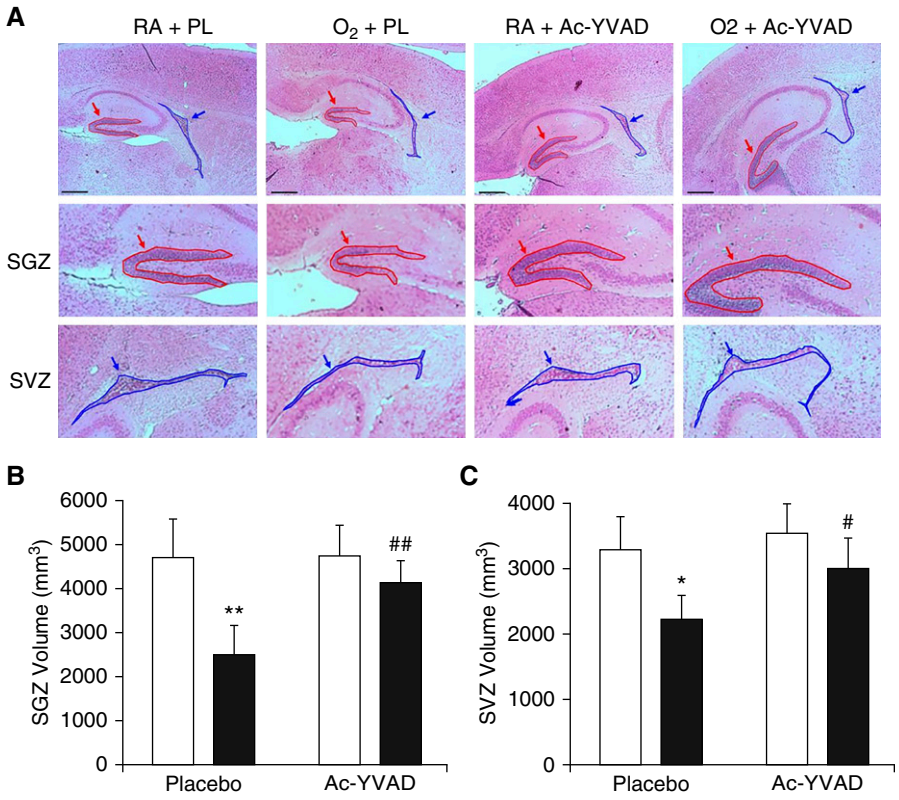

Figure 7. Inhibition of caspase-1 decreases atrophy of the SGZ and subventricularzone (SVZ) of the brain. (*A*) Representative microphotographs of hematoxylin and eosin–stained brain sections taken under 2.5× magnification (unlabeled upper panels), with the red and blue arrows indicating the SGZ and SVZ, respectively, that are enlarged and displayed in the labeled lower panels. (*B*) Measurement of the volume of SGZ showed that it was decreased by hyperoxia plus PL exposure. However, administration of Ac-YVAD-CMK increased the volume of the SGZ in hyperoxia-exposed brains. $^{**}P < 0.01$, RA + PL versus O_2 + PL; $^{\#\#}P < 0.01$, O_2 + PL versus O_2 + Ac-YVAD-CMK. (*C*) Measurement of the volume of SVZ showed that it was decreased by hyperoxia plus PL exposure. However, administration of Ac-YVAD-CMK increased the volume of the SVZ in hyperoxia-exposed brains. $^{*}P < 0.05$, RA + PL versus O_2 + PL, $^{\#}P < 0.05$, O_2 + PL versus O_2 + Ac-YVAD-CMK. Data are presented as mean ± SD; n = 4/group. Open bar: RA; solid bar: 85% O_2. Scale bars: 500 μm.

inflammasome signaling improved alveolarization after 10 days of hyperoxia exposure. Jakkula and coworkers have demonstrated that angiogenesis is necessary for alveolarization during normal lung development, and that injury to the developing pulmonary microvasculature contributes to impaired alveolarization (37). In this study, we found improved vascular density accompanied by improved alveolarization in the Ac-YVAD-CMK–treated hyperoxic pups. Furthermore, these structural changes were associated with increased expression of VEGF and VEGFR2. Vincent and Mohr have shown that inhibition of caspase-1/IL-1β signaling prevents the degeneration of retinal capillaries in diabetes (38). VEGF signaling is impaired in rodents exposed to chronic hyperoxia (39, 40). The disruption of pulmonary VEGF leads to abnormal vascular and alveolar development and lung hypoplasia (41). Lopez-Pastrana and coworkers reported that caspase-1 activation impairs VEGFR2 expression and caspase-1 depletion improves angiogenesis (42). We therefore postulate that the protective effects of Ac-YVAD-CMK in alveolar and vascular development are due to its antiinflammatory effects and ability to augment angiogenesis via caspase-1 inhibition.

A subset of patients with severe BPD develop pulmonary hypertension, characterized by abnormal pulmonary vascular remodeling and tone (43). Pulmonary hypertension occurs in one out of four to five preterm babies with BPD, with a reported mortality of up to 50% (7, 44). Here, we found that inhibition of caspase-1 decreased pulmonary vascular remodeling and right ventricular hypertrophy in hyperoxic animals. These observations, along with our novel finding that antagonism of caspase-1 resulted in increased pulmonary vascular density and decreased pulmonary hypertension, support the hypothesis that targeting NLRP1 inflammasome activation during hyperoxia exposure is key in preserving microvascular development as well as reducing pulmonary hypertension in the developing lung.

There is mounting clinical evidence that severe BPD is an independent risk factor for adverse neurodevelopmental outcomes such as cerebral palsy, impaired cognition, and behavioral disorders, even in the absence of catastrophic brain injuries such as intraventricular hemorrhage (4–6). Despite recent advances in neonatal intensive care and extensive research, the extent to which BPD contributes to neurodevelopmental impairment remains unknown. In this study, we showed that hyperoxia exposure not only induced a BPD-like pathology but also resulted in brain injury in newborn mice. Importantly, we identified a critical role by which caspase-1 mediates hyperoxia activation of the NLRP1 inflammasome in the lung as well as in the brain, and showed that

Figure 6. (Continued). Ac-YVAD-CMK. (*C*) ASC: $^{***}P < 0.001$, RA + PL versus O_2 + PL; $^{\#\#}P < 0.01$, O_2 + PL versus O_2 + Ac-YVAD-CMK. (*D*) Active-Caspase-1: $^{***}P < 0.001$, RA + PL versus O_2 + PL; $^{\#\#\#}P < 0.001$, O_2 + PL versus O_2 + Ac-YVAD-CMK. (*E*) Mature IL-1β: $^{**}P < 0.01$, RA + PL versus O_2 + PL; $^{\#\#}P < 0.01$, O_2 + PL versus O_2 + Ac-YVAD-CMK. (*F*) p53 GSDMD: $^{**}P < 0.01$, RA + PL versus O_2 + PL; $^{\#}P < 0.05$, O_2 + PL versus O_2 + Ac-YVAD-CMK. (*G*) Immunostaining shows that 85% O_2 increased caspase-1, IL-1β, and GSDMD expression in the subgranular zone (SGZ) (brown signal), but treatment with Ac-YVAD-CMK decreased the expression of these factors in the SGZ. Scale bars: 50 μm. Data are shown as mean ± SD. n = 4–6/group. Open bar: RA; solid bar: 85% O_2.

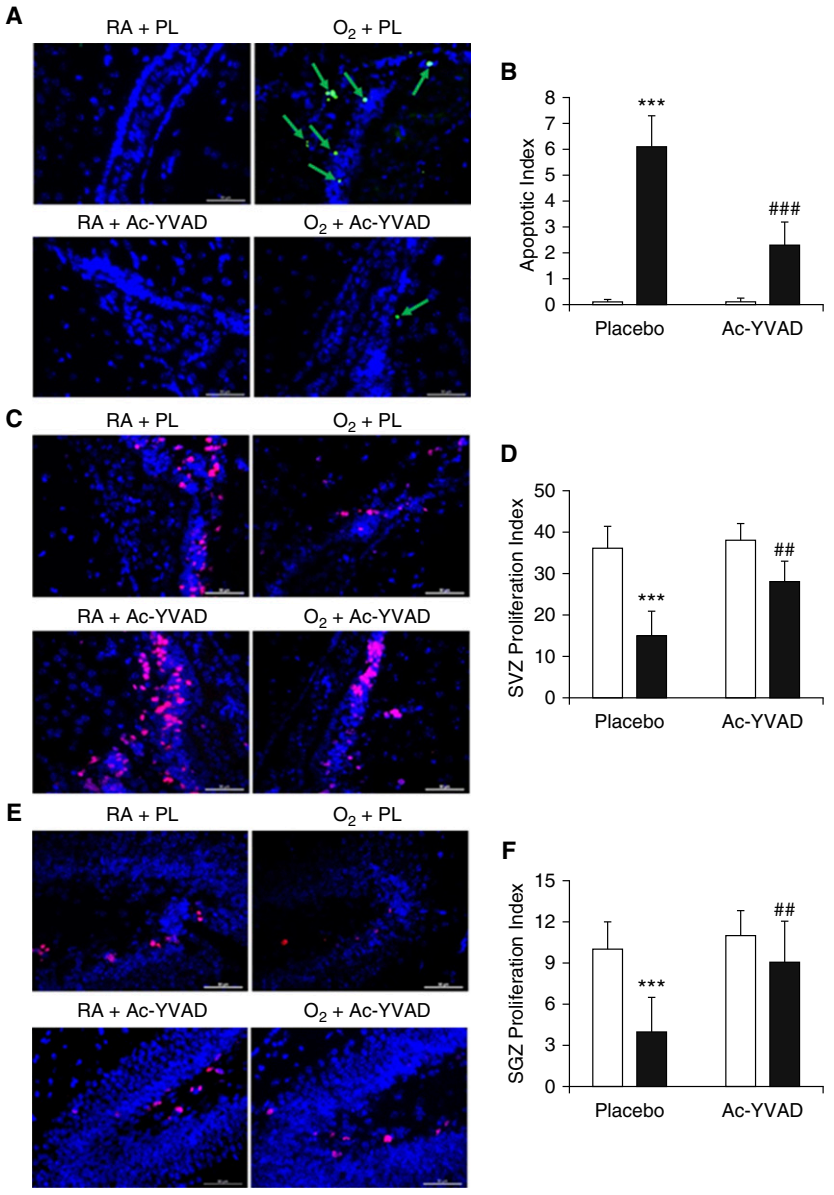

Figure 8. Caspase-1 inhibitor decreases cell death and increases cell proliferation in the brains of hyperoxia-exposed mice. (*A*) Staining with a TUNEL assay (green signals) and DAPI nuclear stain (blue signals) was performed to assess cell death. Representative microphotographs of the SVZ taken under 40× magnification are shown, with the green arrow indicating dead cells. (*B*) Quantification of the cell death index (the percentage of dead nuclei/total nuclei) revealed that hyperoxia exposure in the presence of PL increased the cell death index. However, Ac-YVAD-CMK (Ac-YVAD) decreased the cell death index in the hyperoxic group. $^{***}P < 0.001$, RA + PL versus O_2 + PL, $^{###}P < 0.001$, O_2 + PL versus O_2 + Ac-YVAD-CMK. Data are presented as mean ± SD. (*C*) Immunofluorescent staining for Ki67 (red signals) and DAPI nuclear stain (blue signals) was performed to assess cell proliferation. Representative microphotographs of the SVZ taken under 40× magnification are shown. (*D*) Quantification of the proliferation index (percentage of $Ki67^+$ nuclei/total nuclei) revealed that hyperoxia exposure in the presence of PL decreased the proliferation index. However, Ac-YVAD-CMK increased the proliferation index under hyperoxia. $^{***}P < 0.001$, RA + PL versus O_2 + PL, $^{##}P < 0.01$, O_2 + PL versus O_2 + Ac-YVAD-CMK. (*E*) Cell proliferation assessed by Ki67 (red signals) and DAPI nuclear staining (blue signals). Representative microphotographs of the SGZ taken under 40× magnification are shown. (*F*) Quantification of the proliferation index (the percentage of $Ki67^+$ nuclei/total nuclei) revealed that hyperoxia exposure in the presence of PL decreased the proliferation index. However, treatment with the caspase-1 inhibitor Ac-YVAD-CMK (Ac-YVAD) increased the proliferation index under hyperoxia. $^{***}P < 0.001$, RA + PL versus O_2 + PL, $^{##}P < 0.01$, O_2 + PL versus O_2 + Ac-YVAD-CMK. Data are presented as mean ± SD; $n = 4$/group. Open bar: RA; solid bar: 85% O_2. Scale bars: 50 μm.

inhibition of caspase-1 activity results in attenuated hyperoxia-induced injury in both the lung and brain. More importantly, our findings highlight some of the potential mechanisms through which inhibition of caspase-1 leads to improved lung development and lessened brain atrophy.

In this study, we demonstrated that inhibition of caspase-1 decreased NLRP1 inflammasome activity, which led to reduced active IL-1β in the brain tissues of hyperoxic animals. In addition, we demonstrated for the first time that inhibition of caspase-1 downregulated the expression of p30 GSDMD, an important mediator of pyroptosis in hyperoxia-exposed brain tissues. To further explore whether these molecular changes were associated with reduced brain injury and atrophy, we focused on the SVZ and SGZ of the brain. It is known that the main sites of postnatal neurogenesis in mammals are the SVZ and SGZ of the brain (45–47). In these sites, quiescent NSCs proliferate and generate transit-amplifying neural progenitor cell (NPC) clusters, which further differentiate into astrocytes, oligodendrocytes, and neurons. The SVZ and SGZ are of immense importance because diverse forms of brain injury caused by hypoxia-ischemia are accompanied by stimulation of NSCs in these regions (46, 47). This NSC proliferation is a potential adaptive mechanism to recover from such brain injury. The NPC clusters in the SVZ and SGZ lie in close proximity to blood vessels, which suggests that critical factors from the blood vessels play a role in the proliferation, differentiation, and survival of NPCs (48–50). VEGF promotes the proliferation of endothelial cells and NPCs (51). Hyperoxia exposure downregulates VEGF and VEGFR2 expression in addition to decreasing capillary density in the brain (52). These could account for the increased programmed cell death and decreased proliferation of cells in the SVZ and SGZ during hyperoxia exposure. Furthermore, hyperoxia exposure leads to ROS production in the brain (18), which triggers inflammasome assembly and activation. For these reasons, we evaluated the degree of programmed cell death, cell proliferation, and zonal volumes of the SVZ and SGZ during hyperoxia exposure and administration of the caspase-1 inhibitor. Our study showed that caspase-1 inhibition led to decreased cell death and increased

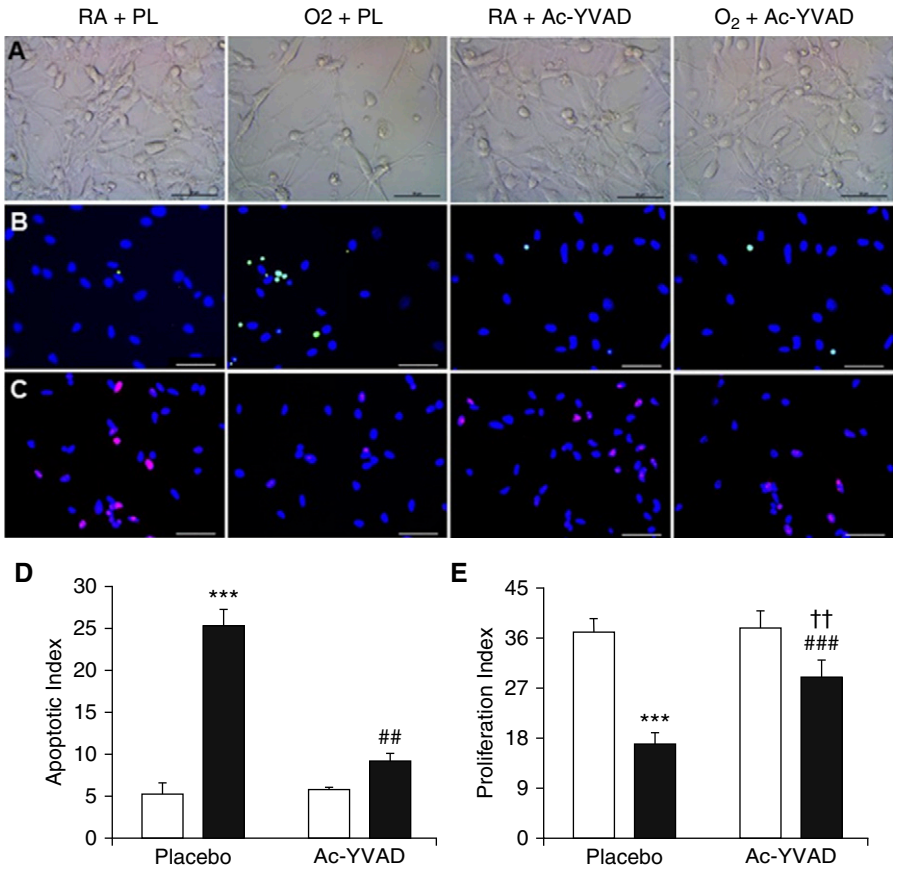

Figure 9. Inhibition of caspase-1 decreases cell death and increases cell proliferation in hyperoxia-exposed neural stem cells (NSCs) in culture. NSCs were exposed to RA or hyperoxia (95% O_2) for 40 hours in the presence of PL or Ac-YVAD-CMK (Ac-YVAD). (*A*) Live cells, phase contrast. (*B*) TUNEL (green) and DAPI nuclear staining (blue) shows (*D*) increased cell death in hyperoxia plus PL–exposed cells, which was decreased by Ac-YVAD-CMK. (*C*) Ki67 staining (pink) and DAPI nuclear staining (blue) show (*E*) decreased cell proliferation in hyperoxia plus PL–treated cells, which was increased by Ac-YVAD-CMK. $^{***}P < 0.001$, RA + PL versus O_2 + PL, $^{\#\#\#}P < 0.001$ and $^{\#\#}P < 0.01$, O_2 + PL versus O_2 + Ac-YVAD-CMK. $^{\dagger\dagger}P < 0.01$, O_2 + Ac-YVAD-CMK versus RA + Ac-YVAD-CMK. Data are presented as mean ± SD; $n = 3$/group. Open bar: RA; solid bar: 95% O_2. Scale bars: 50 μm.

cell proliferation that consequently resulted in improved zonal volumes for the SVZ and SGZ in hyperoxia-exposed brains. Therefore, inhibiting caspase-1 activity may limit the deleterious effects of hyperoxia on the immature brain that are due to activation of the inflammasome and programmed cell death, most likely pyroptosis.

This study also provides *in vitro* evidence that inhibition of capsase-1 is beneficial in preventing hyperoxia-induced NSC injury. In cultured rat fetal NSCs, exposure to 95% oxygen increased cell death, but this effect was blocked by the caspase-1 inhibitor. In addition, hyperoxia also decreased NSC proliferation, and this was partially reversed by caspase-1 inhibition. Thus, these *in vitro* results additionally support the concept that improved NSC survival is likely a major mechanism that contributes to the reduced zonal atrophy by caspase-1 inhibition seen in our hyperoxia neonatal mouse model.

In the present study, we demonstrated concurrent injury to both the lung and the brain during chronic hyperoxia exposure in newborn mice. We demonstrated that hyperoxia upregulated the expression of NLRP1, ASC, active caspase-1, mature IL-1β, and p30 GSDMD in both brain and lung tissues. However, caspase-1 inhibition downregulated the expression of these proteins in the brain and lung of hyperoxia-exposed animals. These findings indicate that the inflammasome is a common signaling pathway that regulates both lung and brain injury in neonates. Although this may be the result of independent direct effects of hyperoxia on both the lung and brain, some studies suggest that lung-to-brain cross-talk (and *vice versa*) mediated by circulating extracellular vesicles (EVs) secreted by both brain and lung cells may also contribute to injury of these two organs (53–61). Neurons, astrocytes, microglia, and oligodendrocytes in the brain have all been reported to secrete caspase-1–containing EVs into the extracellular environment (55–58). Moreover, such brain cell–derived EVs can cross a damaged blood–brain barrier (BBB), as we have recently reported that traumatic brain injury in adult mice releases inflammasome-containing EVs into the serum that target the lung to cause acute lung injury (59). Similarly, oxidative stress, such as occurs in hyperoxia, also causes membrane protein damage that disrupts the BBB and thus may allow EVs to cross the BBB (60). Furthermore, Moon and coworkers have demonstrated that lung epithelial cell–derived, caspase-rich EVs enter the circulation during hyperoxia exposure (61). Accordingly, it is possible that a bidirectional transfer of EVs across the BBB may contribute to the hyperoxic brain and lung injury reported herein.

To the best of our knowledge, this is the first study to demonstrate that hyperoxia activates the inflammasome in both the lung and the brain, and that caspase-1 is a critical factor in regulating hyperoxia-induced lung and brain injury in neonatal mice. Our study has a few limitations. First, we used an extremely high level of oxygen to induce lung injury, which is rarely used clinically in preterm infants. However, this level of oxygen induces lung injury that mimics clinical severe BPD. Second, lung and brain injuries in preterm infants are multifactorial in etiology, and we did not evaluate other contributory factors such as infection and intermittent hypoxia. In addition, brain injury in premature infants is commonly associated with hypoxia/ischemic injury and intraventricular and intraparenchymal brain hemorrhage. It will be important in future studies to explore the role of caspase-1 and inflammasomes in antenatal infection and postnatal moderate hyperoxia-induced injury, as well as intermittent hypoxia-induced lung and brain injury.

In conclusion, in this study we demonstrate that inhibition of caspase-1 largely reversed the injurious effects of

hyperoxia, resulting in attenuated lung inflammation, improved alveolarization and pulmonary vascular development, reduced pulmonary vascular remodeling and right ventricular hypertrophy, and lessened atrophy of the SVZ and SGZ in the brain. Ac-YVAD-CMK was also well tolerated, as we did not observe any deleterious effects of caspase-1 inhibition on measured lung and brain parameters in room air–exposed animals. Although this caspase-1 inhibitor has not been tested in clinical trials, some of the other caspase inhibitors, such as IDN-6556 and PF-03491390, have been used in clinical trials in adult patients with inflammatory liver diseases (62, 63). However, additional studies in neonatal animals are needed to assess the pharmacokinetics and effects on other developing organs before these caspase-1 inhibitors can be used in clinical trials as a novel strategy to prevent and treat lung and brain injury in preterm infants. ■

Author disclosures are available with the text of this article at www.atsjournals.org.

References

1. Stoll BJ, Hansen NI, Bell EF, Shankaran S, Laptook AR, Walsh MC, *et al*.; Eunice Kennedy Shriver National Institute of Child Health and Human Development Neonatal Research Network. Neonatal outcomes of extremely preterm infants from the NICHD Neonatal Research Network. *Pediatrics* 2010;126:443–456.
2. Jobe AH, Bancalari E. Bronchopulmonary dysplasia. *Am J Respir Crit Care Med* 2001;163:1723–1729.
3. Speer CP. Pulmonary inflammation and bronchopulmonary dysplasia. *J Perinatol* 2006;26(Suppl 1):S57–S62; discussion S63–S64.
4. Volpe JJ. Brain injury in premature infants: a complex amalgam of destructive and developmental disturbances. *Lancet Neurol* 2009;8: 110–124.
5. Schmidt B, Asztalos EV, Roberts RS, Robertson CM, Sauve RS, Whitfield MF; Trial of Indomethacin Prophylaxis in Preterms (TIPP) Investigators. Impact of bronchopulmonary dysplasia, brain injury, and severe retinopathy on the outcome of extremely low-birth-weight infants at 18 months: results from the trial of indomethacin prophylaxis in preterms. *JAMA* 2003;289:1124–1129.
6. Trittmann JK, Nelin LD, Klebanoff MA. Bronchopulmonary dysplasia and neurodevelopmental outcome in extremely preterm neonates. *Eur J Pediatr* 2013;172:1173–1180.
7. Herbert S, Tulloh R. Sildenafil, pulmonary hypertension and bronchopulmonary dysplasia. *Early Hum Dev* 2016;102:21–24.
8. Cayabyab RG, Jones CA, Kwong KYC, Hendershott C, Lecart C, Minoo P, *et al*. Interleukin-1β in the bronchoalveolar lavage fluid of premature neonates: a marker for maternal chorioamnionitis and predictor of adverse neonatal outcome. *J Matern Fetal Neonatal Med* 2003;14: 205–211.
9. Rindfleisch MS, Hasday JD, Taciak V, Broderick K, Viscardi RM. Potential role of interleukin-1 in the development of bronchopulmonary dysplasia. *J Interferon Cytokine Res* 1996;16: 365–373.
10. Nold MF, Mangan NE, Rudloff I, Cho SX, Shariatian N, Samarasinghe TD, *et al*. Interleukin-1 receptor antagonist prevents murine bronchopulmonary dysplasia induced by perinatal inflammation and hyperoxia. *Proc Natl Acad Sci USA* 2013;110:14384–14389.
11. Howrylak JA, Nakahira K. Inflammasomes: key mediators of lung immunity. *Annu Rev Physiol* 2017;79:471–494.
12. He WT, Wan H, Hu L, Chen P, Wang X, Huang Z, *et al*. Gasdermin D is an executor of pyroptosis and required for interleukin-1β secretion. *Cell Res* 2015;25:1285–1298.
13. Liao J, Kapadia VS, Brown LS, Cheong N, Longoria C, Mija D, *et al*. The NLRP3 inflammasome is critically involved in the development of bronchopulmonary dysplasia. *Nat Commun* 2015;6:8977.
14. Hummler JK, Dapaah-Siakwan F, Vaidya R, Zambrano R, Luo S, Chen S, *et al*. Inhibition of rac1 signaling downregulates inflammasome activation and attenuates lung injury in neonatal rats exposed to hyperoxia. *Neonatology* 2017;111:280–288.
15. Vaidya R, Zambrano R, Hummler JK, Luo S, Duncan MR, Young K, *et al*. Recombinant CCN1 prevents hyperoxia-induced lung injury in neonatal rats. *Pediatr Res* 2017;82:863–871.
16. Felderhoff-Mueser U, Sifringer M, Polley O, Dzietko M, Leineweber B, Mahler L, *et al*. Caspase-1-processed interleukins in hyperoxia-induced cell death in the developing brain. *Ann Neurol* 2005;57: 50–59.
17. Hoehn T, Felderhoff-Mueser U, Maschewski K, Stadelmann C, Sifringer M, Bittigau P, *et al*. Hyperoxia causes inducible nitric oxide synthase-mediated cellular damage to the immature rat brain. *Pediatr Res* 2003;54:179–184.
18. Felderhoff-Mueser U, Bittigau P, Sifringer M, Jarosz B, Korobowicz E, Mahler L, *et al*. Oxygen causes cell death in the developing brain. *Neurobiol Dis* 2004;17:273–282.
19. Ray AM, Owen DE, Evans ML, Davis JB, Benham CD. Caspase inhibitors are functionally neuroprotective against oxygen glucose deprivation induced CA1 death in rat organotypic hippocampal slices. *Brain Res* 2000;867:62–69.
20. Sozen T, Tsuchiyama R, Hasegawa Y, Suzuki H, Jadhav V, Nishizawa S, *et al*. Role of interleukin-1beta in early brain injury after subarachnoid hemorrhage in mice. *Stroke* 2009;40:2519–2525.
21. Hummler SC, Rong M, Chen S, Hehre D, Alapati D, Wu S. Targeting glycogen synthase kinase-3β to prevent hyperoxia-induced lung injury in neonatal rats. *Am J Respir Cell Mol Biol* 2013;48: 578–588.
22. Arnon S, Grigg J, Silverman M. Pulmonary inflammatory cells in ventilated preterm infants: effect of surfactant treatment. *Arch Dis Child* 1993;69:44–48.
23. Kotecha S, Wilson L, Wangoo A, Silverman M, Shaw RJ. Increase in interleukin (IL)-1 β and IL-6 in bronchoalveolar lavage fluid obtained from infants with chronic lung disease of prematurity. *Pediatr Res* 1996;40:250–256.
24. Merritt TA, Cochrane CG, Holcomb K, Bohl B, Hallman M, Strayer D, *et al*. Elastase and alpha 1-proteinase inhibitor activity in tracheal aspirates during respiratory distress syndrome: role of inflammation in the pathogenesis of bronchopulmonary dysplasia. *J Clin Invest* 1983;72:656–666.
25. Groneck P, Götze-Speer B, Oppermann M, Eiffert H, Speer CP. Association of pulmonary inflammation and increased microvascular permeability during the development of bronchopulmonary dysplasia: a sequential analysis of inflammatory mediators in respiratory fluids of high-risk preterm neonates. *Pediatrics* 1994;93: 712–718.
26. Menzel M, Akbarshahi H, Mahmutovic Persson I, Puthia M, Bjermer L, Uller L. Caspase-1 deficiency reduces eosinophilia and interleukin-33 in an asthma exacerbation model. *ERJ Open Res* 2017;3:pii: 00047-02017.
27. Freeman BA, Topolosky MK, Crapo JD. Hyperoxia increases oxygen radical production in rat lung homogenates. *Arch Biochem Biophys* 1982;216:477–484.
28. Stogner SW, Payne DK. Oxygen toxicity. *Ann Pharmacother* 1992;26: 1554–1562.
29. Mantell LL, Horowitz S, Davis JM, Kazzaz JA. Hyperoxia-induced cell death in the lung–the correlation of apoptosis, necrosis, and inflammation. *Ann N Y Acad Sci* 1999;887:171–180.
30. Nakahira K, Haspel JA, Rathinam VA, Lee SJ, Dolinay T, Lam HC, *et al*. Autophagy proteins regulate innate immune responses by inhibiting the release of mitochondrial DNA mediated by the NALP3 inflammasome. *Nat Immunol* 2011;12:222–230.
31. Juliana C, Fernandes-Alnemri T, Kang S, Farias A, Qin F, Alnemri ES. Non-transcriptional priming and deubiquitination regulate NLRP3 inflammasome activation. *J Biol Chem* 2012;287: 36617–36622.

32. Cruz CM, Rinna A, Forman HJ, Ventura AL, Persechini PM, Ojcius DM. ATP activates a reactive oxygen species-dependent oxidative stress response and secretion of proinflammatory cytokines in macrophages. *J Biol Chem* 2007;282:2871–2879.
33. Abais JM, Xia M, Zhang Y, Boini KM, Li P-L. Redox regulation of NLRP3 inflammasomes: ROS as trigger or effector? *Antioxid Redox Signal* 2015;22:1111–1129.
34. Martinon F. Signaling by ROS drives inflammasome activation. *Eur J Immunol* 2010;40:616–619.
35. Jin C, Flavell RA. Molecular mechanism of NLRP3 inflammasome activation. *J Clin Immunol* 2010;30:628–631.
36. Thébaud B, Abman SH. Bronchopulmonary dysplasia: where have all the vessels gone? Roles of angiogenic growth factors in chronic lung disease. *Am J Respir Crit Care Med* 2007;175:978–985.
37. Jakkula M, Le Cras TD, Gebb S, Hirth KP, Tuder RM, Voelkel NF, *et al*. Inhibition of angiogenesis decreases alveolarization in the developing rat lung. *Am J Physiol Lung Cell Mol Physiol* 2000;279: L600–L607.
38. Vincent JA, Mohr S. Inhibition of caspase-1/interleukin-1beta signaling prevents degeneration of retinal capillaries in diabetes and galactosemia. *Diabetes* 2007;56:224–230.
39. Maniscalco WM, Watkins RH, D'Angio CT, Ryan RM. Hyperoxic injury decreases alveolar epithelial cell expression of vascular endothelial growth factor (VEGF) in neonatal rabbit lung. *Am J Respir Cell Mol Biol* 1997;16:557–567.
40. Hosford GE, Olson DM. Effects of hyperoxia on VEGF, its receptors, and HIF-2α in the newborn rat lung. *Am J Physiol Lung Cell Mol Physiol* 2003;285:L161–L168.
41. Grover TR, Parker TA, Zenge JP, Markham NE, Kinsella JP, Abman SH. Intrauterine hypertension decreases lung VEGF expression and VEGF inhibition causes pulmonary hypertension in the ovine fetus. *Am J Physiol Lung Cell Mol Physiol* 2003;284:L508–L517.
42. Lopez-Pastrana J, Ferrer LM, Li YF, Xiong X, Xi H, Cueto R, *et al*. Inhibition of caspase-1 activation in endothelial cells improves angiogenesis: a novel therapeutic potential for ischemia. *J Biol Chem* 2015;290:17485–17494.
43. Khemani E, McElhinney DB, Rhein L, Andrade O, Lacro RV, Thomas KC, *et al*. Pulmonary artery hypertension in formerly premature infants with bronchopulmonary dysplasia: clinical features and outcomes in the surfactant era. *Pediatrics* 2007;120:1260–1269.
44. Mourani PM, Sontag MK, Younoszai A, Miller JI, Kinsella JP, Baker CD, *et al*. Early pulmonary vascular disease in preterm infants at risk for bronchopulmonary dysplasia. *Am J Respir Crit Care Med* 2015;191: 87–95.
45. Porzionato A, Macchi V, Zaramella P, Sarasin G, Grisafi D, Dedja A, *et al*. Effects of postnatal hyperoxia exposure on the rat dentate gyrus and subventricular zone. *Brain Struct Funct* 2015;220: 229–247.
46. Yang Z, Levison SW. Hypoxia/ischemia expands the regenerative capacity of progenitors in the perinatal subventricular zone. *Neuroscience* 2006;139:555–564.
47. Jin K, Minami M, Lan JQ, Mao XO, Batteur S, Simon RP, *et al*. Neurogenesis in dentate subgranular zone and rostral subventricular zone after focal cerebral ischemia in the rat. *Proc Natl Acad Sci USA* 2001;98:4710–4715.
48. Palmer TD, Willhoite AR, Gage FH. Vascular niche for adult hippocampal neurogenesis. *J Comp Neurol* 2000;425:479–494.
49. Shen Q, Wang Y, Kokovay E, Lin G, Chuang SM, Goderie SK, *et al*. Adult SVZ stem cells lie in a vascular niche: a quantitative analysis of niche cell-cell interactions. *Cell Stem Cell* 2008;3:289–300.
50. Tavazoie M, Van der Veken L, Silva-Vargas V, Louissaint M, Colonna L, Zaidi B, *et al*. A specialized vascular niche for adult neural stem cells. *Cell Stem Cell* 2008;3:279–288.
51. Jin K, Zhu Y, Sun Y, Mao XO, Xie L, Greenberg DA. Vascular endothelial growth factor (VEGF) stimulates neurogenesis *in vitro* and *in vivo*. *Proc Natl Acad Sci USA* 2002;99:11946–11950.
52. Benderro GF, Sun X, Kuang Y, Lamanna JC. Decreased VEGF expression and microvascular density, but increased HIF-1 and 2α accumulation and EPO expression in chronic moderate hyperoxia in the mouse brain. *Brain Res* 2012;1471:46–55.
53. Pelosi P, Rocco PR. The lung and the brain: a dangerous cross-talk. *Crit Care* 2011;15:168.
54. Winklewski PJ, Radkowski M, Demkow U. Cross-talk between the inflammatory response, sympathetic activation and pulmonary infection in the ischemic stroke. *J Neuroinflammation* 2014;11:213.
55. Perregaux D, Barberia J, Lanzetti AJ, Geoghegan KF, Carty TJ, Gabel CA. IL-1 beta maturation: evidence that mature cytokine formation can be induced specifically by nigericin. *J Immunol* 1992;149: 1294–1303.
56. Chivet M, Hemming F, Pernet-Gallay K, Fraboulet S, Sadoul R. Emerging role of neuronal exosomes in the central nervous system. *Front Physiol* 2012;3:145.
57. Frühbeis C, Fröhlich D, Kuo WP, Amphornrat J, Thilemann S, Saab AS, *et al*. Neurotransmitter-triggered transfer of exosomes mediates oligodendrocyte-neuron communication. *PLoS Biol* 2013;11: e1001604.
58. Qu Y, Franchi L, Nunez G, Dubyak GR. Nonclassical IL-1 beta secretion stimulated by P2X7 receptors is dependent on inflammasome activation and correlated with exosome release in murine macrophages. *J Immunol* 2007;179:1913–1925.
59. Kerr NA, de Rivero Vaccari JP, Abbassi S, Kaur H, Zambrano R, Wu S, *et al*. Traumatic brain injury-induced acute lung injury: evidence for activation and inhibition of a neural-respiratory-inflammasome axis. *J Neurotrauma* 2018;35:2067–2076.
60. Pun PBL, Lu J, Moochhala S. Involvement of ROS in BBB dysfunction. *Free Radic Res* 2009;43:348–364.
61. Moon H-G, Cao Y, Yang J, Lee JH, Choi HS, Jin Y. Lung epithelial cell-derived extracellular vesicles activate macrophage-mediated inflammatory responses via ROCK1 pathway. *Cell Death Dis* 2015;6: e2016.
62. Baskin-Bey ES, Washburn K, Feng S, Oltersdorf T, Shapiro D, Huyghe M, *et al*. Clinical trial of the pan-caspase inhibitor, IDN-6556, in human liver preservation injury. *Am J Transplant* 2007;7:218–225.
63. Shiffman ML, Pockros P, McHutchison JG, Schiff ER, Morris M, Burgess G. Clinical trial: the efficacy and safety of oral PF-03491390, a pancaspase inhibitor—a randomized placebo-controlled study in patients with chronic hepatitis C. *Aliment Pharmacol Ther* 2010;31: 969–978.